Title

MOLECULAR AUTOIONIZATION LIFETIMES AND CROSS SECTIONS FOR PENNING IONIZATION: NUMERICAL RESULTS FOR He* (ls2s 3s) +H(ls S)

Authors

Miller, W.H.
Slocomb, C.A.
Schaefer, Henry F.

Publication Date

1971-06-01

Submitted to Chemical Physics

UCRL-20709
Preprint

MOLECULAR AUTOIONIZATION LIFETIMES AND CROSS SECTIONS FOR PENNING IONIZATION: NUMERICAL RESULTS FOR $He^*(1s2s\ ^3S) + H(1s\ ^2S)$

W. H. Miller, C. A. Slocomb and Henry F. Schaefer III

June 1971

AEC Contract No. W-7405-eng-48

LAWRENCE RADIATION LABORATORY
UNIVERSITY of CALIFORNIA BERKELEY

DISCLAIMER

MOLECULAR AUTOIONIZATION LIFETIMES AND CROSS SECTIONS FOR PENNING IONIZATION: NUMERICAL RESULTS FOR $He^*(1s2s\ ^3S) + H(1s\ ^2S)$ †

W. H. Miller** and C. A. Slocomb

Inorganic Materials Research Division, Lawrence Radiation Laboratory
Department of Chemistry, University of California
Berkeley, California 94720

and

Henry F. Schaefer III

Department of Chemistry, University of California
Berkeley, California 94720

ABSTRACT

The width Γ (or lifetime $\hbar/\Gamma$) for autoionization of $He^*(1s2s\ ^3S) + H(1s\ ^2S)$ has been calculated as a function of internuclear distance, and cross sections for Penning and associative ionization ($He^* + H \rightarrow He + H^+ + e^-$, $HeH^+ + e^-$) have been determined for low collision energies. Associative ionization is 22% of the total ionization cross section in the limit of zero collision energy; this fraction decreases with increasing energy, being $\sim$18% at a collision energy corresponding to 300°K. The distribution in energy of the ionized electron is also calculated, and it is suggested that measurement of this quantity should lead to a good estimate of the well-depth of the He^*-H potential. Comparison of these results to those obtained by an orbitting model shows that the model (suitably scaled) is adequate in predicting the total ionization cross section, but is less accurate for the more detailed collision properties.

† Supported by the University of California Committee on Research, the Petroleum Research Fund, the Research Corporation, and the U. S. Atomic Energy Commission.

** Alfred P. Sloan Fellow.

I. INTRODUCTION

Of various collision processes which involve electronic transitions, Penning ionization[1] (PI)

$$A^* + B \rightarrow A + B^+ + e^- \qquad (1)$$

is one of the simplest from a theroretical point of view, the reason being that it takes place within the Born-Oppenheimer approximation for the separation of electronic and nuclear motion. [In Eq.(1)A^* is an electronically excited state of species A, and the excitation energy of $A \rightarrow A^*$ must be greater than the ionization potential of species B.] Thus at each internuclear distance the initial electronic state A^*-B finds itself embedded on a continuum of electronic states of the type $A\text{-}B^+ + e^-$ and therefore undergoes autoionization with some characteristic rate; this is a simple example of a discrete→continuum "golden-rule", or "radiationless" transition.[2]

Because of the resonant nature of the transition, cross sections for PI may be appreciable,[3,4] on the order of 10's of $Å^2$; non-resonant electronic transitions are typically an order of magnitude smaller. Thus PI can be an important process in atmospheric chemistry and physics,[5,6] particularly so if the electronically excited species A^* is metastable (i.e., cannot decay radiatively by optically allowed transitions); in this case Eq. (1) may be the key process which determines the steady-state concentration of species A^*.

The metastable states of helium ($1s2s\,^1S, ^3S$) have received most attention with regard to PI, both experimentally[3,4,7] and theoretically[8-15] for (1) they are sufficiently energetic (∿19-20 eV) to ionize almost any collision partner, (2) helium is an important constituent of the atmosphere,

(3) the radiative lifetime of these states is long enough for them to be studied under a variety of experimental conditions, and (4) helium is sufficiently simple electronically to allow theoretical treatments from first principles. The simplest collision partner being the hydrogen atom, the particular process

$$He(1s2s\ ^3S) + H(1s\ ^2S) \rightarrow He(1s^2\ ^1S) + H^+ + e^-(^2S) \qquad (2)$$

has been the subject of several recent theoretical studies, and experimental results have also been reported for the macroscopic rate constant. More details of the collision dynamics will presumably be available soon from molecular beam type measurements.

In a previous paper[15] we reported accurate calculations for the diatomic potential curves which pertain to the process in Eq. (2), and a simple orbitting model[10] was employed to obtain the various cross sections; this model did not require knowledge of the autoionization rate. This present paper reports the calculation of the autoionization rate[16] as a function of internuclear distance. With this quantity it is now possible to evaluate quite rigorously the various collision properties of interest: the total ionization cross section, the relative amount of associated (HeH^+) and dissociated ($He+H^+$) product, the energy and/or angular distribution of the ionized electron, and the angular distribution of the heavy particles.

Section II discusses the calculation of the autoionization rate, and Section III summarizes the necessary cross section formulas. Section IV presents results for the total ionization cross section as a function of collision energy, the relative amount of associated and

dissociated product, and the energy distribution of the ionized electron. Comparison of these collision properties with those given by the orbitting model of reference 15 shows that the model gives good results at low collision energy for the total ionization cross section (if it is scaled appropriately), but is poorer with regard to the more detailed collision properties. Isotope effects within this "scaled orbitting model" are considered in the Appendix, and it is predicted that the total ionization cross section for He^{*} + D is 10% greater than that for He^{*} + H.

II. CALCULATION OF THE AUTOIONIZATION RATE

Any rigorous evaluation of cross sections for PI requires knowledge of the autoionization rate, or width of the initial electronic state as a function of internuclear distance. Calculation of the width is an electronic structure problem which lies within the Born-Oppenheimer approximation. With the nuclei held fixed, therefore, autoionization of the electronic state of the "diatomic molecule" A-B which dissociates to A^*+B is no different from autoionization of an atom (except, of course, in the lack of spherical symmetry).

A. Theoretical Considerations

It has been shown[17,18] that quite accurate autoionization widths can be obtained by the "golden-rule"-like expression

$$\Gamma = 2\pi\rho \, |\langle \chi | H-E | \psi \rangle|^2 \qquad (3)$$

where Γ is the autoionization width (units of energy), ψ is the initial (discrete) electronic state, χ is the final (continuum) electronic state which is energetically degenerate with ψ, H is the total electronic Hamiltonian, E is the electronic energy of the discrete state, and ρ is the density of final continuum states (which is determined by the way χ is normalized asymptotically). Equation (3) is expected[18] to be most accurate for autoionization of a neutral species, leaving a positively charged fragment; this is, of course, the case for PI.

For our calculation the discrete electronic function ψ is a configuration interaction (CI) type of wavefunction (normalized to unity).

$$\psi(1,2,\cdots,N) = \sum_{K_N} C(K_N) \, |K_N\rangle \quad , \qquad (4)$$

where $|K_N\rangle = |k_1,k_2,\cdots,k_N\rangle$ denotes an N-electron normalized Slater determinant

$$|K_N\rangle = (N!)^{-1/2} \det|\phi_{k_1}(1)\phi_{k_2}(2)\cdots\phi_{k_N}(N)|, \tag{5}$$

$\{\phi_k\}$ being the orthogonal molecular orbitals; the coefficients $C(K_N)$ are determined by diagonalizing the matrix $\langle K_N'|H|K_N\rangle$ and choosing the particular eigenfunction and eigenvalue which dissociate to A^*+B as the internuclear distance $R\to\infty$.

For the continuum function first consider χ in the form

$$\chi(1,2,\cdots,N) = N^{1/2}\, \Phi_+(1,2,\cdots,N-1)\phi_{\vec{\varepsilon}}(N), \tag{6}$$

where Φ_+ is the electronic wavefunction of the (N-1)-electron molecular ion $A\text{-}B^+$ and $\phi_{\vec{\varepsilon}}$ is the continuum orbital ($\vec{\varepsilon}$ denotes the asymptotic energy ε and direction $\hat{\varepsilon}$ of the ionized electron); Φ_+ is also a CI type wavefunction (normalized to unity)

$$\Phi_+(1,2,\cdots,N-1) = \sum_{K_{N-1}} C^{(+)}(K_{N-1})|K_{N-1}\rangle , \tag{7}$$

where $|K_{N-1}\rangle \equiv |k_1,k_2,\cdots,k_{N-1}\rangle$ is an (N-1)-electron normalized Slater determinant. [The coefficients $C^{(+)}(K_{N-1})$ are similarly determined by diagonalizing the (N-1)-electron Hamiltonian on the $|K_{N-1}\rangle$ basis.] The purpose of the factor $N^{1/2}$ in Eq. (6) is so that the resulting width has the factor N :

$$\Gamma = 2\pi\rho\, N|\langle \Phi_+\phi_{\vec{\varepsilon}}|H-E|\psi\rangle|^2 \quad . \tag{8}$$

Equation (8) without the factor of N would be appropriate if only the N^{th} electron could autoionize; since ψ is totally antisymmetric in all N electrons, however, any one of the N electrons may autoionize, and the width is thus N times larger.

Rather than using Eq. (8), a more symmetrical (and more useful) form is obtained by taking the continuum function as

$$\chi(1,2,\cdots,N) = \sum_{K_{N-1}} C^{(+)}(K_{N-1})|\bar{K}_N\rangle , \tag{9}$$

where $|\bar{K}_N\rangle$ is the N-electron Slater determinant

$$|\bar{K}_N\rangle = (N!)^{-1/2}\det|\phi_{k_1}(1)\phi_{k_2}(2)\cdots\phi_{k_{N-1}}(N-1)\phi_{\vec{\varepsilon}}(N)| \tag{10}$$

in which the N^{th} orbital for each configuration is the continuum orbital. By noting that

$$\langle \bar{K}_N|H-E|K_N'\rangle \equiv \int d\tau_N (N!)^{-1/2}\det|\phi_{k_1}^*(1)\cdots\phi_{k_{N-1}}^*(N-1)\phi_{\vec{\varepsilon}}^*(N)|$$

$$(H-E)(N!)^{-1/2}\det|\phi_{k_1'}(1)\cdots\phi_{k_N'}(N)|$$

$$= \int d\tau_N\, N(N!)^{-1/2}\det|\phi_{k_1}^*(1)\cdots\phi_{k_{N-1}}^*(N-1)|\phi_{\vec{\varepsilon}}^*(N)$$

$$(H-E)(N!)^{-1/2}\det|\phi_{k_1'}(1)\cdots\phi_{k_N'}(N)|$$

$$= N^{1/2}\int d\tau_N[(N-1)!]^{-1/2}\det|\phi_{k_1}^*(1)\cdots\phi_{k_{N-1}}^*(N-1)|\phi_{\vec{\varepsilon}}^*(N)$$

$$(H-E)(N!)^{-1/2}\det|\phi_{k_1'}(1)\cdots\phi_{k_N'}(N)|,$$

one sees that χ in Eq. (9) gives the same result for Γ as does the form of χ in Eq. (6). This latter form [Eq. (9)], however, being the sum of N-electron Slater determinants (as is ψ) means that the matrix element $\langle\chi|H-E|\psi\rangle$ can be computed by standard methods; this is also true only because the <u>same molecular orbitals</u> were used to construct the CI

expansion for Φ_+ as for ψ. Had this not been done, one would have the difficult task of evaluating matrix elements between determinants with non-orthogonal orbitals.

For the continuum orbital $\phi_{\vec{\varepsilon}}(\vec{r})$ we use a coulomb function centered on nucleus B; this is obviously a realistic description of the continuum electron when it is not too close to the nuclei, and the width expression is known[18] to be insensitive to the nature of the continuum function close in.

As mentioned above, our standard routines for evaluating matrix elements between N-electron Slater determinants can be employed only if all the orbitals are mutually orthogonal. If M bound-state molecular orbitals $\{\phi_{k_i}\}$, i=1,$\cdots$,M are used in constructing ψ and Φ_+, therefore, the actual continuum orbital we use is the function $\bar{\phi}_{\vec{\varepsilon}}$

$$\bar{\phi}_{\vec{\varepsilon}} \equiv \phi_{\vec{\varepsilon}} - \sum_{i=1}^{M} \phi_{k_i} \langle \phi_{k_i} | \phi_{\vec{\varepsilon}} \rangle \tag{11}$$

It is clear that $\bar{\phi}_{\vec{\varepsilon}}$ is orthogonal to all the bound-state orbitals and also that the asymptotic normalization of $\bar{\phi}_{\vec{\varepsilon}}$ is the same as that of the original continuum orbital $\phi_{\vec{\varepsilon}}$ (for all the bound-state orbitals vanish exponentially in the asymptotic region). One may question whether this modification of the continuum orbital caused by orthogonalizing it to all the bound-state orbitals will affect the value obtained for Γ; the answer is "no" and can be seen in the following manner: Modifying the continuum orbital as in Eq. (11) modifies the function χ similarly,

$$\chi = \bar{\chi} + \Delta\chi \tag{12}$$

where χ is the continuum function if $\phi_{\vec{\varepsilon}}$ is used as the continuum orbital and $\bar{\chi}$ is the continuum function if the orthogonalized function

$\bar{\phi}^{\rightarrow}_{\varepsilon}$ is used as the continuum orbital; $\Delta\chi$ is given explicitly by

$$\Delta\chi = \sum_{j=1}^{M} \langle \phi_{k_j} | \phi^{\rightarrow}_{\varepsilon} \rangle \sum_{K_{N-1}} C^{(+)}(K_{N-1}) | K_N^{(j)} \rangle \ , \tag{13}$$

where $|K_N^{(j)}\rangle \equiv |k_1, k_2, \cdots, k_{N-1}, k_j\rangle$. The difference in the discrete-continuum matrix element which results from using χ or $\bar{\chi}$ is thus

$$\langle \Delta\chi | H-E | \psi \rangle = \sum_{j=1}^{M} \langle \phi^{\rightarrow}_{\varepsilon} | \phi_{k_j} \rangle \sum_{K_{N-1}} C^{(+)}(K_{N-1})$$

$$\sum_{K_N'} \langle K_N^{(j)} | H-E | K_N' \rangle \, C(K_N'), \tag{14}$$

where $K_N' = (k_1', k_2', \cdots, k_N')$ and $K_N^{(j)} = (k_1, k_2, \cdots, k_{N-1}, k_j)$. But the coefficients $C(K_N')$ satisfy the homogeneous equations

$$\sum_{K_N'} \langle K_N^{(j)} | H-E | K_N' \rangle \, C(K_N') = 0 \tag{15}$$

for all Slater determinants $|K_N^{(j)}\rangle$ which are included on the CI expansion of ψ. Since we carried out[15] a <u>complete</u> CI for our chosen set of molecular orbitals, <u>all</u> $|K_N^{(j)}\rangle$ are included in the expansion of ψ, so that each term in the sum over j in Eq. (14) is zero; thus

$$\langle \Delta\chi | H-E | \psi \rangle = 0,$$

and this proves that the matrix element $\langle \chi | H-E | \psi \rangle$ is unchanged by using the orthogonalized continuum orbital $\bar{\phi}^{\rightarrow}_{\varepsilon}$ in place of the original one $\phi^{\rightarrow}_{\varepsilon}$.

To see how the argument proceeds if one carries out less than a complete CI expansion for ψ, note that Eq. (15) can also be written as

$$\sum_{K_N'} \langle K_N^{(j)}|H-E|K_N'\rangle\, C(K_N') = \langle K_N^{(j)}|H-E|\psi\rangle = 0. \qquad (15')$$

If $|K_N^{(j)}\rangle$ is one of the configurations included in ψ, then (as before) Eq. (15') is satisfied. If $|K_N^{(j)}\rangle$ is a configuration which was not included in ψ, however, the quantity in Eq. (15') must still be essentially zero--or else one should re-do the CI calculation for ψ and include this configuration; i.e., the matrix element in Eq. (15') is the measure of how much a configuration $|K_N^{(j)}\rangle$ "mixes" with ψ and is thus the normal criterion for whether or not it should be included in the CI expansion of ψ. One concludes, therefore, that to the extent that all "important" configurations have been included in the CI expansion for ψ, the matrix element $\langle\chi|H-E|\psi\rangle$ is unchanged by orthogonalizing the original continuum orbital $\phi_\varepsilon^{\rightarrow}$ to all the bound-state orbitals [as is done in Eq. (11)].

Finally, we conclude this sub-section by noting that one will ordinarily employ a partial wave expansion for the continuum orbital $\phi_\varepsilon^{\rightarrow}(\vec{r})$,

$$\phi_\varepsilon^{\rightarrow}(\vec{r}) = \sum_{\ell m} Y_{\ell m}^{*}(\hat{\varepsilon})\, i^{\ell} e^{i\sigma_\ell}\, \phi_{\varepsilon\ell m}(\vec{r}), \qquad (16)$$

where σ_ℓ is the coulomb phase shift[19] and the continuum orbital $\phi_{\varepsilon\ell m}$ is

$$\phi_{\varepsilon\ell m}(r) = \frac{1}{r}\, F_\ell(-1/k_\varepsilon,\, k_\varepsilon r)\, Y_{\ell m}(\hat{r}), \qquad (17)$$

and $k_\varepsilon = (2\varepsilon)^{1/2}$ is the asymptotic momentum of the continuum electron (atomic units being used, $\hbar = m_e = 1$). The angles $\hat{\varepsilon}$ and $\hat{r}$ are referred to the internuclear axis. The coulomb radial function F_ℓ is normalized at large r as[19]

$$F_\ell\,(-1/k_\varepsilon, k_\varepsilon r) \sim \sin[k_\varepsilon r + \frac{1}{k_\varepsilon}\,\ell n(2k_\varepsilon r) - \pi\ell/2 + \sigma_\ell],$$

and with this normalization the density of continuum states is such that in atomic units

$$2\pi\rho = 4/k_\varepsilon.$$

The width for autoionization in direction $\hat{\varepsilon}$ with respect to the internuclear axis is thus[20]

$$\Gamma(\vec{\varepsilon}) = 2\pi\rho\Big|\sum_\ell Y_{\ell m}(\hat{\varepsilon})\; i^{-\ell}\; e^{i\sigma_\ell}\; I_\ell\Big|^2, \tag{17}$$

where

$$I_\ell = \langle \chi_{\varepsilon\ell m}|H - E|\psi\rangle \tag{18}$$

and $\chi_{\varepsilon\ell m}$ is given by Eq. (9) with the continuum orbital now being $\phi_{\varepsilon\ell m}(\vec{r})$ [actually it is $\bar{\phi}_{\varepsilon\ell m}(\vec{r})$ which has been orthogonalized to the bound-state orbitals as in Eq. (11)]. Since the component of electronic orbital angular momentum along the internuclear axis is a good quantum number, only one value of m contributes to the sum in Eq. (17), namely the value $m = \Lambda_o - \Lambda_+$, where Λ_o and Λ_+ are the usual Λ-quantum numbers

for the state A^{*} -B and A $-B^{+}$, respectively (i.e., Λ = 0, 1, 2 ... is denoted by Σ, Π, Δ, ...); all values of $\ell \geq |m|$ contribute to the sum. [Note that since only one value of m contributes to the sum in Eq. (17), the angular dependence of $\Gamma(\vec{\epsilon})$ is such that it depends only on the angle between $\hat{\epsilon}$ and $\hat{R}$.] The value of ϵ is fixed by energy conservation

$$\epsilon = \epsilon(R) \equiv V_o(R) - V_+(R), \tag{19}$$

V_o and V_+ being the electronic energy of A^{*} -B and A $-B^{+}$ at internuclear distance R. [Fig. 1 shows these potential curves for He^{*} -H and He $-H^{+}$.] The total width

$$\Gamma \equiv \int d_2 \hat{\epsilon}\, \Gamma(\hat{\epsilon}) \tag{20}$$

is easily evaluated from Eq. (17) and seen to be the sum of all partial widths

$$\Gamma = \sum_{\ell=|m|}^{\infty} \Gamma_\ell, \tag{21}$$

where

$$\Gamma_\ell = 2\pi\rho\, |I_\ell|^2. \tag{22}$$

In sub-section c it will be seen how one can estimate the number of terms that are required for convergence of this sum.

B. Numerical Methods

The task, then, is to compute the matrix elements I_ℓ defined by Eq. (18). In terms of I_ℓ Eq. (17) gives the width for autoionization in any direction, and Eqs. (21) and (22) give the total width.

Since the CI calculations for wavefunctions ψ and Φ_+ have been carried out previously[15] and the coefficients $C(K_N)$ and $C^{(+)}(K_{N-1})$ thus determined, the problem reduces to that of evaluating one- and two-electron integrals of the types

$$[i|\ell] = \int d\tau_1 \, \phi_i^*(1) \left[-\frac{Z_A}{r_A} - \frac{Z_B}{r_B} - 1/2 \, \nabla^2 \right] \phi_{\varepsilon\ell m}(1)$$

$$[ij|k\ell] = \int d\tau_1 \int \phi\tau_2 \, \phi_i^*(1)\phi_j(1) \left[\frac{1}{r_{12}}\right] \phi_k^*(2) \, \phi_{\varepsilon\ell m}(2).$$

The bound-state orbitals $\{\phi_i\}$ are normalized Slater functions times spherical harmonics, and the continuum orbital $\phi_{\varepsilon\ell m}(\vec{r})$ is the coulomb function of Eq. (17). For some test calculations a plane wave was used for the continuum orbital; the only modification in this case is that the coulomb radial function is replaced in Eq. (17) by a spherical Bessel function:

$$F_\ell(-1/k_\varepsilon, k_\varepsilon r) \to k_\varepsilon r \, j_\ell(k_\varepsilon r).$$

There are a number of methods available for the evaluation of one- and two-electron integrals involving Slater functions.[21-27] Since these methods make explicit use of the analytical properties of the Slater functions, however, they cannot be directly used to evaluate

integrals of the above types containing the continuum orbital $\phi_{\varepsilon \ell m}$. In addition, the ℓ values for the continuum function can take on rather high values (up to $\ell = 9$ were necessary in the present work) and the derivation of special analytic formulas for different ℓ values would be extremely tedious.

The conceptually simplest way of evaluating integrals of the above type is via a completely numerical procedure which does not depend on the analytic properties of either the bound-state or continuum orbitals. With calculations of this type in mind, such a procedure has been implemented and reported in the literature.[28] Essentially the only change required in our standard program[28] was the addition of subroutines to evaluate the particular type of continuum function being used to describe the ejected electron. We also found that it was necessary to change the numerical integration grids fairly drastically to allow for the fact that the integrands are much more diffuse than in standard electronic structure problems.

The fact that the integral evaluation scheme was essentially identical to that thoroughly tested for bound-state calculations[29] reduced the possibility of error. However, a second test of the method was carried out. For this purpose the fact was used that the total width Γ [given by Eq. (21)] obtained by using a plane wave continuum orbital will be independent of the point in space at which the orbital is centered. The width Γ was calculated with the plane wave centered at both the He and H nuclei for internuclear separation 4.0 bohrs, and the two widths obtained were identical to 3 significant figures.

C. Results for He^* ($1s2s\ ^3S$) + H($1s\ ^2S$) and Comparison with Previous Work

Figs. 2 and 3 show our results for the matrix elements $I_\ell(R)$ and the total width $\Gamma(R)$, respectively,

$$\Gamma(R) = (4/k_\varepsilon) \sum_{\ell=0}^{\infty} |I_\ell(R)|^2, \tag{23}$$

$$(1/2)k_\varepsilon^2 = \varepsilon = V_o(R) - V_+(R), \tag{24}$$

V_o and V_+ being the He^* -H and He -H^+ potential curves computed previously [15] and shown in Fig. 1. Table I gives the numerical values corresponding to Figs. 2 and 3.

One notices that the matrix elements I_ℓ oscillate with ℓ and that the number of partial waves required increases with increasing internuclear distance R. Both of these features can be understood by noting that on the basis of electron spin considerations,

$$He^*(\uparrow\uparrow) + H(\downarrow) \rightarrow He(\uparrow\downarrow) + H^+ + e^-(\uparrow),$$

the ejected electron must "come from" helium. The continuum orbital, however, is a coulomb function centered on H, so that the matrix element $I_\ell(R)$ can be expected to be roughly proportional to the amplitude of the coulomb function at the He center,

$$I_\ell(R) \sim F_\ell(-1/k_\varepsilon, k_\varepsilon R).$$

For fixed ℓ this is an oscillatory function of R, and for fixed R, it oscillates with ℓ. The function takes on its maximum value (in an absolute value sense) when R and ℓ are related by the classical turning point criterion

$$(1/2)k_\varepsilon^2 = -1/R + \ell^2/2R^2,$$

or

$$\ell_{max} = (k_\varepsilon^2 R^2 + 2R)^{1/2}.$$

Thus $I_\ell(R)$ oscillates with ℓ for $\ell < \ell_{max}$, takes on its maximum value for $\ell \sim \ell_{max}$, and then decreases exponentially for $\ell > \ell_{max}$.

In Fig. 3 are also shown the results of Bell[14] for the total width as a function of internuclear distance; there is rough qualitative agreement. Apart from the use of much less sophisticated wavefunctions for He^* -H and He $-H^+$, there are several other approximations incorporated in these calculations. Bell[14] uses as continuum orbital a coulomb function centered on H (as do we), but for all R takes ε, the energy of the ejected electron, to be that appropriate to $R \simeq \infty$, namely $\varepsilon = V_o(\infty) - V_+(\infty) \simeq .233$ hartree $\simeq 6.06$ eV. The correct value $\varepsilon(R) = V_o(R) - V_+(R)$ varies considerably with R, as seen in Fig. 4, being 9.09 eV at $R = 2\ a_o$ and 4.34 eV at $R = 4\ a_o$, for example, with our calculated potential curves. Even more serious, however, is the fact that only terms $\ell = 0$ and 1 were included in the partial wave summation for Γ; as seen in Fig. 2, this is clearly insufficient even for $R = 2\ a_o$.

Fujii et al.[12] have also computed $\Gamma(R)$ within a similar framework as that of Bell[14]: the continuum orbital is a coulomb function centered on H with ε taken as $V_o(\infty) - V_+(\infty)$, and they included partial waves $\ell = 0, 1, 2$. Their results appear to be similar to those of Bell[14], but it is difficult to tell accurately from their figure.

III. CROSS SECTION FORMULAS

There have been a number of theoretical descriptions[8-15,30-35] of collisional autoionization (of which PI is an example); our notation follows the formulation of Ref. 35. The most detailed cross section possible is that which is differential in the scattering angle of the heavy particles and also differential in the energy and angle of the ionized electron, $\sigma(\vec{\epsilon}, \hat{k}_f)$; less detailed cross sections are partial integrals of this. The energy distribution of the electron, for example, is

$$\sigma(\epsilon) = \int d_2\hat{\epsilon} \int d_2\hat{k}_f \, \sigma(\vec{\epsilon}, \hat{k}_f),$$

and the total ionization cross section is

$$\sigma = \int d\epsilon \, \sigma(\epsilon) = \int d_3\vec{\epsilon} \int d_2\hat{k}_f \, \sigma(\vec{\epsilon}, \hat{k}_f).$$

The quantum mechanical expression for the cross section is the square modules of an amplitude

$$\sigma(\vec{\epsilon}, \hat{k}_f) = |f(\vec{\epsilon}, \hat{k}_f \leftarrow o, \hat{k}_o)|^2,$$

where o denotes the initial electronic state A^*-B, $\vec{k}_o$ is the initial relative momentum vector of A^* and B, $\vec{\epsilon}$ is the energy and direction of the ionized electron, and $\vec{k}_f$ is the final relative momentum vector of A and B^+; energy conservation requires that

$$\hbar^2 k_o^{\,2}/2\mu + \Delta = \hbar^2 k_f^{\,2}/2\mu + \varepsilon,$$

where μ is the reduced mass of A and B, and Δ is the difference in the excitation energy $A \rightarrow A^*$ and the ionization potential of B. The scattering amplitude, exact within the Born-Oppenheimer approximation, is given by[30]

$$f(\vec{\varepsilon},\hat{k}_f \leftarrow o,\hat{k}_o) = -\frac{1}{4\pi}\frac{2\mu}{\hbar^2}(k_f/k_o)^{1/2}\frac{1}{4\pi}\rho_\varepsilon^{\,1/2}$$

$$\int d_3\vec{R}\; u_{\vec{k}_f}^{(-)}(\vec{R})^*\; V_{\vec{\varepsilon},o}(\vec{R})\; u_{\vec{k}_o}^{(+)}(\vec{R}),$$

where the electronic matrix element is the quantity discussed in Section IIa

$$V_{\vec{\varepsilon},o}(\vec{R}) = \langle \chi_{\vec{\varepsilon}}|H - E|\psi\rangle$$

$$= \sum_\ell Y_{\ell m}(\hat{\varepsilon}\; V\; \hat{R})\; i^{-\ell}\; e^{i\sigma_\ell}\langle \chi_{\varepsilon\ell m}|H-E|\psi\rangle,$$

except that now ε and R are independent of one another; $\hat{\varepsilon}\; V\; \hat{R}$ denotes the angles $\hat{\varepsilon}$ with respect to $\hat{R}$ and ρ_ε is the density of continuum electronic states. The functions $u_{\vec{k}_o}(\vec{R})$ and $u_{\vec{k}_f}(\vec{R})$ are the scattering functions (normalized as plane waves) which result for the spherically symmetric potentials $V_o(R) - i\Gamma(R)/2$ and $V_+(R)$, respectively; the + and - denote the usual outgoing and incoming boundary conditions.

Classical and semiclassical approximations may be developed from this quantum expression.[35] Within these approximations there is a

correlation between ε, the energy of the ionized electron, and R, the internuclear distance at which ionization takes place,

$$\varepsilon = V_o(R) - V_+(R); \tag{25}$$

Fig. 4 shows this function for the He^* + H case. For fixed ε, therefore, autoionization must occur at $R(\varepsilon)$, the root of Eq. (25) [note that there may be more than one such root]. If autoionization occurs at internuclear distance R, however, one knows the classical deflection function associated with the heavy particle trajectory:

$$\Theta_{in}(\ell,R) = \pi - \ell \int_R^\infty dR' \, [R'^2 \, k_o(R')]^{-1}$$

$$- \ell \int^R dR' \, [R'^2 \, k_f(R')]^{-1} - \ell \int^\infty dR' \, [R'^2 \, k_f(R')]^{-1} \tag{26}$$

$$\Theta_{out}(\ell,R) = \pi - \ell \int^\infty dR' [R'^2 k_o(R')]^{-1} - \ell \int^R dR' [R'^2 k_o(R')]^{-1}$$

$$- \ell \int_R^\infty dR' \, [R'^2 \, k_f(R')]^{-1}, \tag{27}$$

where ℓ is the orbital angular momentum for relative motion of A and B (which is conserved), $k_o(R)$ and $k_f(R)$ are the local momenta in $V_o(R)$ and $V_+(R)$, "in" and "out" refer to whether auotionization occurs on the inward or outward part of the radial motion, and the unspecified lower limits of the integrals are the classical turning points. From these deflection functions one can easily construct the angular distribution for the heavy particles which corresponds to an ionized electron energy

of ε. From Eq. (17) one, in addition, knows the angular distribution of the electrons with respect to the instantaneous internuclear axis. Thus the completely differential cross section is given classically by

$$\sigma(\vec{\varepsilon},\hat{k_f}) \equiv \sigma(\varepsilon,\theta_\varepsilon,\phi_\varepsilon,\theta,\phi)$$

$$= \sigma_{in}(\varepsilon,\theta_\varepsilon,\phi_\varepsilon,\theta,\phi) + \sigma_{out}(\varepsilon,\theta_\varepsilon,\phi_\varepsilon,\theta,\phi) \qquad (28)$$

where

$$(\varepsilon,\theta_\varepsilon,\phi_\varepsilon) \equiv \vec{\varepsilon} \quad \text{and} \quad (\theta,\phi) \equiv \hat{k_f}, \quad \text{and}$$

$$\sigma_{in}(\varepsilon,\theta_\varepsilon,\phi_\varepsilon,\theta,\phi) = b\left[\sin\theta\left|\frac{\partial\Theta_{in}(b,R)}{\partial b}\right| \; |\varepsilon'(R)|\right]^{-1}$$

$$\times \frac{\Gamma(R,\hat{\varepsilon}\cdot\hat{R})}{\hbar v_b(R)} \; \exp\left[-\int_R^\infty dR' \; \Gamma(R')/\hbar v_b(R')\right] \qquad (29)$$

where R is evaluated at the root of Eq. (25). In Eqs. (28) and (29) the deflection function Θ_{in} is considered as a function of the initial impact parameter $b \equiv \ell/k_o$, rather than ℓ, and b is evaluated at the root of

$$\Theta_{in}(b,R) = \pm\,\theta.$$

[If there are multiple roots for b and/or R, then Eq. (29) is a sum of such terms, one for each pair of roots (b,R).] The direction $\hat{R}$ in Eq. (29) is that of the internuclear axis at the instant of autoionization; thus $\hat{R} = (\theta_{in},\phi)$, where

$$\theta_{in} = \ell \int_R^\infty dR' \; [R'^2 k_o(R')]^{-1} \quad ;$$

$\Gamma(R,\hat{\varepsilon}\cdot\hat{R})$ is the function from Eq. (17), and

$$\hat{\varepsilon}\cdot\hat{R} = \cos\theta_\varepsilon \cos\theta_{in} + \sin\theta_\varepsilon \sin\theta_{in} \cos(\phi_\varepsilon - \phi).$$

One sees that the aximuthal dependence of $\sigma(\vec{\varepsilon},\hat{k_f})$ only involves the difference of azimuthal angles (ϕ_ε,ϕ). A similar expression gives $\sigma_{out}(\varepsilon,\theta_\varepsilon,\phi_\varepsilon,\theta,\phi)$, the modifications of Eq. (29) being

$$\theta_{in} \to \theta_{out}$$

$$\theta_{in} \to \theta_{out}$$

$$\exp[-\int_R^\infty dR'\ \Gamma(R')/\hbar v_b(R')] \to \exp[-\int^\infty dR'\ \Gamma(R')/\hbar v_b(R')$$

$$-\int^R dR'\ \Gamma(R')/\hbar v_b(R')]\ ,$$

where

$$\theta_{out} = \ell\int^\infty dR'[R'^2 k_o(R')]^{-1} + \ell \int^R dR'[R'^2 k_o(R')]^{-1};$$

the unspecified lower limit of the integrals is the classical turning point.

The two quantities for which we present numerical results in the next section are the total ionization cross section

$$\sigma = 2\pi \int_o^\infty db\ b\ P_b, \tag{30}$$

and the energy distribution of the ionized electron

$$\sigma(\varepsilon) = 2\pi \int_o^\infty db\ b\ P_b(R)\ |\varepsilon'(R)|^{-1} \tag{31}$$

where $P_b(R)dR$ is the probability that (for impact parameter b) auto-ionization takes place in the interval (R, R+dR),

$$P_b(R) = [\Gamma(R)/\hbar v_b(R)] \exp[-\int^{\infty} dR' \, \Gamma(R')/\hbar v_b(R')]$$

$$\times 2\cosh[\int^{R} dR' \, \Gamma(R')/\hbar v_b(R')], \qquad (32)$$

and P_b is the total probability of autoionization for impact parameter b,

$$P_b = \int^{\infty} dR \, P_b(R),$$

or one finds that

$$P_b = 1 - \exp[-2 \int^{\infty} dR' \, \Gamma(R')/\hbar v_b(R')]; \qquad (33)$$

$v_b(R)$ is the local velocity,

$$v_b(R) = v_o[1-V_o(R)/E-b^2/R^2]^{1/2},$$

v_o being the initial asymptotic velocity. Since $\varepsilon(R) = V_o(R) - V_+(R)$ is not monotonic (see Fig. 4), there are typically two values of R which satisfy Eq. (25), so that $P_b(R)$ is the sum of two terms, one for each root.

As discussed previously,[35] the classical expression for $\sigma(\varepsilon)$ fails for ε near ε_*, the minimum of $\varepsilon(R)$ (see Fig. 4). The appropriate semi-classical extension has been developed for ε near ε_*, and this corresponds to modifying Eq. (31) by the replacement[36]

$$|\varepsilon'(R)|^{-1} \rightarrow (\hbar v_*)^{-1/3}(2/\varepsilon_*'')^{2/3} \, 2\pi \, Ai^2(-z) \qquad (34)$$

where

$$\varepsilon_*'' = \varepsilon''(R_*),$$

R_* being that value of R for which $\varepsilon'(R) = 0$; also

$$v_* = v_b(R_*)$$

$$z = (\hbar v_*)^{-2/3}(2/\varepsilon_*'')^{1/3}(\varepsilon-\varepsilon_*).$$

Finally, although it does not apply in the He^* + H case, we note that if the transition is <u>weak</u> (i.e., if $P_b << 1$ for all b), then Eq. (32) becomes

$$P_b(R) \simeq \Gamma(R)/\hbar v_b(R),$$

and then the integral over b in Eq. (31) can be carried out; this gives the following explicit expression for $\sigma(\varepsilon)$

$$\sigma(\varepsilon) = |\varepsilon'(R)|^{-1}\, 4\pi R^2[\Gamma(R)/\hbar v_o](1-V_o(R)/E)^{1/2}$$

where R is evaluated at the root of Eq. (25). The total ionization cross section is given in this case by

$$\sigma = \int^{\infty} dR\, 4\pi R^2\, [\Gamma(R)/\hbar v_o][1-V_o(R)/E]^{1/2}.$$

IV. CROSS SECTIONS FOR $He^*(1s2s\ ^3S) + H(1s\ ^2S)$

For the case $He^*(1s2s\ ^3S) + H(1s\ ^2S)$ all of the cross section formulas of the preceding section must be multiplied by 1/3; this is a purely statistical factor[10] that accounts for the fact that of the six spin states arising from $He^*(^3S) + H(^2S)$, four are components of $^4\Sigma$ He^*-H and cannot autoionize, while two are components of $^2\Sigma$ He^*-H and do autoionize.

A. Total Ionization Cross Sections

Figure 5 shows the total ionization cross section [computed from Eqs. (30) and (33)] as a function of initial translational energy. Also shown is the fraction of this which results in associated product, HeH^+, this process being associative ionization (AI). The cross section for AI was determined by assuming that all resonant states of HeH^+ are associated; i.e., tunneling was neglected. [See the discussion of this point in references 15 and 35.] Figure 6 shows the percentage of associated product as a function of collision energy.

Since $V_o(R)$ for He^*-H is strongly attractive and since we are considering the region of low collision energy, the integral over b in Eq. (30) has a sharp cut-off at B, that value at which classical orbitting occurs. This is true because the outermost classical turning point in $V_o(R)$ jumps discontinuously from small R to large R at b = B; since $\Gamma(R)$ decreases exponentially with R, P_b drops essentially to zero for b > B. Furthermore, the transition probability P_b is almost independent of b for b < B, being equal essentially to its b = 0 value; for low energies it is also independent of E. This results because the contribution to the integral over R' in Eq. (33) comes dominantly from

the turning point region, and for low energy and a strong attractive interaction the turning point varies only slightly with b and E before the orbitting cut-off. With these approximations Eqs. (30) and (33) give

$$\sigma = \frac{1}{3}\sigma_{orbit}\, P_o \tag{35}$$

where

$$\sigma_{orbit} = \pi B^2 \tag{36}$$

$$P_o = 1 - \exp\{-(2\mu/\hbar^2)^{1/2} \int_{R_o}^{\infty} dr'\, \Gamma(R')[-V_o(R')]^{-1/2}\} \tag{37}$$

i.e., P_o is P_b of Eq. (33) for the case b = E = 0. From our potential $V_o(R)$ and $\Gamma(R)$ we find

$$P_o \simeq 0.789, \tag{38}$$

and $\sigma_{orbit}(E)$ has been computed previously.[15]

The dashed lines in Fig. 5 are the results of the "scaled orbitting model", Eqs. (35)-(38). It is seen that it gives excellent results for the total ionization cross section, but is rather poor for predicting σ_{AI}, the fraction of the total that is associated product. This failure is due to the fact that determination of σ_{AI} requires that the model specify at what value of R autoionization occurs; this detail of the dynamics is not required for the total ionization cross section. The orbitting model of reference 15 assumes that autoionization takes place only at the classical turning point, and this appears to be unrealistically restrictive. Autoionization actually occurs for all classically allowed values of R with varying probability, and this autoionization at larger values of R reduces σ_{AI} considerably below that predicted by the orbitting model.

To illustrate this feature more clearly, Figure 7 shows the quantity $P_o(R)$ - i.e., the function $P_b(R)$ of Eq. (32) for the case $b = E = 0$. Figure 8 shows its indefinite integral $\tilde{P}_o(R)$,

$$\tilde{P}_o(R) = \int_{R_o}^{R} dR' \, P_o(R') \tag{39}$$

$$= (1-P_o)^{1/2} \, 2 \sinh\left[\int_{R_o}^{R} dR' \, \Gamma(R')/\hbar v_o(R')\right]; \tag{40}$$

$\tilde{P}_o(R)$ is the probability that autoionization occurs for an internuclear distance less than or equal to R. Figures 7 and 8 show that although most autoionization does take place at small R, a significant amount occurs at distances away from the classical turning point; the orbitting model would give $\tilde{P}_o(R)$ as a step-function

$$\tilde{P}_o(R) = P_o \, h[R-R_o],$$

R_o being the turning point. The difference between these two distributions of autoionization probability has important consequences for the amount of associated product because the turning point in the He^*-H potential is high up on the outer wall of the $He-H^+$ potential well (see Fig. 1).

With the function $\tilde{P}_o(R)$ of Eq. (39) and Fig. 8 it is easy to determine the fraction of associated product in the limit of zero collision energy. As $E \to 0$, only $b = 0$ contributes, the orbitting cut-off prohibiting contribution from other impact parameters. For $b = 0$, however, autoionization at internuclear distance R will result in associated product if, and only if,

$$V_+(R) + V_o(\infty) - V_o(R) < V_+(\infty),$$

or

$$\varepsilon(R) > \varepsilon(\infty). \tag{41}$$

If R_{AI} is that finite value of R for which $\varepsilon(R) = \varepsilon(\infty)$ [see Fig. 4], then

$$\lim_{E\to 0} \sigma_{AI}/\sigma_{tot} = \int_{R_o}^{R_{AI}} dR\, P_o(R) / \int_{R_o}^{\infty} dR\, P_o(R)$$

or

$$\lim_{E\to 0} \sigma_{AI}/\sigma_{tot} = \tilde{P}_o(R_{AI})/\tilde{P}_o(\infty). \tag{42}$$

Since $R_{AI} \simeq 2.49\ a_o$ (see Fig. 4), one finds from Fig. 8 that the fraction of associated product in the limit of zero collision energy is ∿22%. [The orbitting model would predict the fraction to be 100%.] Since $\tilde{P}_o(R)$ rises rapidly to its asymptotic value as R increases (see Fig. 8) and since the value of R_{AI} is a sensitive function of the potential curves, this limiting fraction of AI is a sensitive function of the shape of $V_o(R)$ and $V_+(R)$, primarily in the region about the zero energy turning point of $V_o(R)$.

The results of Fujii et al.[12] for the total ionization cross section agree well with our results in Fig. 5 at the lower range of energies, but decrease faster at higher energies, being 7 $Å^2$ at 0.8 eV, compared to 12 $Å^2$ in Fig. 5. Bell[14] obtains a thermally averaged cross section of 28 $Å^2$ at T = 300°K, compared to a value of 33 $Å^2$ from Fig. 5 at E = 0.03 eV. The flowing afterglow measurements of Shaw et al.[37] give an average cross section of (22 ± 6) $Å^2$ at T = 300°K, and the major product is found to be $He + H^+$, although HeH^+ is also found. Our results (Fig. 6) at E = 0.03 eV gives 18% HeH^+ and 82% $He + H^+$ as the product distribution, in qualitative agreement with these measurements.

B. Energy Distribution of the Ionized Electron

Figures 9-11 show $\sigma(\varepsilon)$, the distribution in energy of the ionized electron, for typical "low", "medium", and "high" collision energies E = 0.01 eV, 0.03 eV, and 0.136 eV, respectively. The classical expression [Eq. (31) and (32)] was used, and the semiclassical modification given by Eq. (34) for ε near ε_* is shown by dashed lines.

The dominant feature in $\sigma(\varepsilon)$ is the maximum near ε_*; although the classical infinity is removed by Eq. (34), the peak is still prominent, increasing in height as the collision energy decreases. For the present case of He^* and H, the difference between $\varepsilon_* \simeq 4.32$ eV and the asymptotic value $\varepsilon(\infty) \simeq 6.06$ eV is a rough measure of the well-depth of $V_o(R)$ [the He^*-H potential]. This follows because $V_+(R)$ [the He-H^+ potential] is of much shorter range than $V_o(R)$, being only slightly different from its asymptotic value at the minimum of $V_o(R)$ (cf. Fig. 1). For our potentials $\varepsilon(\infty) - \varepsilon_* = 1.74$ eV, and the well-depth of $V_o(R)$ is 1.91 eV. Measurement of $\sigma(\varepsilon)$, therefore, should give important information about the depth of the He^*-H potential well. It should be noted, however, that the maximum in $\sigma(\varepsilon)$ does not occur precisely at ε_*; thus it would be necessary to fit the peak to the Airy function form in Eq. (34) in order to extract ε_*.

At low collision energies (i.e., Figs. 9 and 10) two other peaks appear in $\sigma(\varepsilon)$, these at larger ε. The origin of these features can be seen by considering the limit of $\sigma(\varepsilon)$ as $E \to 0$. As discussed above, only b=0 contributes in this limit, so that

$$\sigma(\varepsilon) \sim P_o(R)/|\varepsilon'(R)| \equiv P_o(\varepsilon), \tag{43}$$

where $P_o(R)$ is given by Eq. (37) and shown in Fig. 7, and R is the root of $\varepsilon(R) = \varepsilon$; $P_o(\varepsilon)$ is shown in Fig. 12. The singularity in $P_o(\varepsilon)$ at $\varepsilon \simeq 7.43$ eV corresponds to $R = R_o$, the root of $V_o(R) = V_o(\infty)$; i.e., this is the "turning-point singularity" that is present in $P_o(R)$ (cf. Fig. 7) because only b = 0 contributes. For small but non-zero collision energy, a small range of impact parameters contributes to the integral over b in Eq. (31), and this averages out the turning-point singularity; the peaks in $\sigma(\varepsilon)$ at $\varepsilon \simeq 7$ eV in Fig. 9 and $\varepsilon \simeq 6.3$ eV in Fig. 10, however, are the remnant of this singularity. It is seen that this peak is shifted to progressively smaller ε as the collision energy increases, as well as being rapidly reduced in height; it is completely absent in Fig. 11 (E = 0.136 eV).

The other peak in Fig. 12 is located at $\varepsilon = \varepsilon(\infty) \simeq 6.06$ eV and is due to a large contribution from large values of R because $|\varepsilon'(R)| \to 0$ as $R \to \infty$. Although it is true that

$$\lim_{R\to\infty} [\Gamma(R)/\hbar v_b(R)]/|\varepsilon'(R)| = 0,$$

our potential curves and width give a region of large R for which $|\varepsilon'(R)|$ decreases faster than $\Gamma(R)/\hbar v_b(R)$, giving rise to this sharp spike near $\varepsilon(\infty)$. [Actually, the stationary phase approximation used[35] to obtain the classical expression for $\sigma(\varepsilon)$ from the quantum one fails if $\varepsilon'(R) \to 0$; a more refined semiclassical treatment for ε near $\varepsilon(\infty)$, therefore, would round-off this spike somewhat.] This peak in $\sigma(\varepsilon)$ also diminishes as the collision energy increases (only a faint shoulder remains in Fig. 11), but its position remains fixed at $\varepsilon(\infty)$.

Finally, we note that the scaled orbitting model (i.e., the results from Eq. (6) of reference 15 multiplied by $\frac{1}{3} P_o = 0.263$) gives poor agreement with the results in Figs. 9-11, due again to the fact that it requires that autoionization occur while the atoms are at a classical turning point of their relative motion. The model gives better agreement with Eqs. (31) and (32) for higher collision energies ($E \gtrsim 0.4$ eV); for energies $E \gtrsim 1$ eV, however, the model begins to fail even for the total ionization cross section (as seen in Fig. 5), so that the range of its utility regarding $\sigma(\varepsilon)$, $0.4 \text{ eV} \lesssim E \lesssim 1$ eV, is quite limited.

APPENDIX: Isotope Effects

Here we consider the total ionization cross section, defined by Eqs. (30) and (33), as a function of initial translational energy E and the reduced mass of the atoms μ. If the transition is weak (i.e., $P_b \ll 1$ for all b), then it has been shown[35] that

$$\sigma(\mu,E) = \mu^{1/2} \times \text{function } (E) \tag{A1}$$

so that if different isotopic species of the same atoms are studied, one has

$$R \equiv \sigma(\mu_2,E)/\sigma(\mu_1,E) = (\mu_2/\mu_1)^{1/2}. \tag{A2}$$

For He^*-H (isotope number 1) and He^*-D (isotope number 2), for example, the cross section ratio would be $(5/3)^{1/2} \simeq 1.29$, a 30% effect.

The case of He^*-H however, is not that of a weak transition; because of the strong attractive interaction, however, the orbitting model discussed in Section IV is valid at low energy. From Eqs. (35)-(37), therefore,

$$\sigma(\mu,E) = \frac{1}{3}\sigma_{orbit}(E)\,[1-\exp(-c\mu^{1/2})], \tag{A3}$$

where it has been noted that the cross section for orbitting is independent of μ and that c is independent of μ and E. The cross section ratio in this case thus becomes

$$R = [1-\exp(-c\mu_2^{1/2})]/[1-\exp(-c\mu_1^{1/2})]. \tag{A4}$$

As $c \to \infty$, $R \to 1$ (the strong limit), and as $c \to 0$, $R \to (\mu_2/\mu_1)^{1/2}$ (the weak limit).

One will generally not be able to calculate the constant c in order to predict the cross-section ratio, the only prediction being that R lies between 1 and $(\mu_2/\mu_1)^{1/2}$. If <u>three</u> isotopic variants are observed, however, then measurement of the cross section for 1 and 2 will determine c via Eq. (A4), so that the cross section for isotope number 3 will be predicted. From another point of view, measurement of the cross section ratio in Eq. (A4) determines the constant c and thus determines the effective transition probability in Eq. (A3).

Finally, for He^*-H we found in Section IV an effective transition probability of 0.789, which gives $c \simeq 1.740\ (\text{amu})^{-1/2}$; this predicts the cross section ratio for He^*-D to He^*-H to be $R \simeq 1.10$, a 10% effect.

REFERENCES

1. For a recent review, see E. E. Muschlitz, Jr. Adv. Chem. Phys. 10, 171 (1966).

2. See, for example, L. I. Schiff, Quantum Mechanics (McGraw-Hill, N. Y. 1968) pp. 283-285.

3. A. L. Schmeltekopf and F. C. Fehsenfeld, J. Chem. Phys. 53, 3173 (1970).

4. R. C. Bolden, R. S. Hemsworth, M. J. Shaw, and N. D. Twiddy, J. Phys. B, 3, 61 (1970).

5. E. E. Ferguson and H. Schlüter, Planet. Space Sci. 9, 701 (1962).

6. See also, A. Dalgarno, Adv. Atom. Mol. Phys. 4, 381 (1968).

7. See also the first 15 references of reference 3.

8. O. von Roos, J. Chem. Phys. 30, 729 (1959).

9. E. E. Ferguson, Phys. Rev. 128, 210 (1962).

10. D. R. Bates, K. L. Bell, and A. E. Kingston, Proc. Phys. Soc. (London) 91, 288 (1967).

11. K. L. Bell, A. Dalgarno, A. E. Kingston, J. Phys. B 1, 18 (1968).

12. H. Fujii, H. Nakamura, and M. Mori, J. Phys. Soc. Japan 29, 1030 (1970).

13. M. Matsuzawa and K. Katsuura, J. Chem. Phys. 52, 3001 (1970).

14. K. L. Bell, J. Phys. B 3, 1308 (1970).

15. W. H. Miller and H. F. Schaefer, J. Chem. Phys. 53, 1421 (1970).

16. Γ, units of energy, is the width of the autoionizing state, $\Gamma/\hbar$ is the rate of autoionization, and $\hbar/\Gamma$ is the lifetime with respect to autoionization.

17. W. H. Miller, Phys. Rev. 152, 70 (1966).

18. W. H. Miller, Chem. Phys. Letters 4, 627 (1970).

19. M. Abramowitz and I. A. Stegun, Handbook of Mathematical Functions (U. S. Government Printing Office, Washington, 1964), pp. 537-543.

20. The phase is $i^{-\ell}$, rather than i^{ℓ}, because of outgoing boundary conditions on $\phi^{\rightarrow}_{\varepsilon}$.

21. K. Ruedenberg, J. Chem. Phys. 19, 1459 (1951).

22. F. E. Harris, J. Chem. Phys. 32, 3 (1960).

23. I. Shavitt and M. Karplus, J. Chem. Phys. 36, 550 (1962).

24. M. P. Barnett, Methods in Computational Physics, 2, 95 (1963).

25. A. C. Wahl, P. E. Cade, and C. C. J. Roothaan, J. Chem. Phys. 41, 2578 (1964).

26. A. D. McLean and M. Yoshimine, IBM J. Res. Develop. 12, 206 (1968).

27. H. J. Silverstone, J. Chem. Phys. 48, 4098 (1968).

28. H. F. Schaefer, J. Chem. Phys. 52, 6241 (1970).

29. H. F. Schaefer, J. Chem. Phys. 54, 2207 (1971).

30. T. F. O'Malley, Phys. Rev. 150, 14 (1966).

31. A. Herzenberg, Phys. Rev. 160, 80 (1967).

32. J. C. Y. Chen, Phys. Rev. 156, 12 (1967).

33. M. Mori, J. Phys. Soc. Japan 26, 773 (1969).

34. H. Nakamura, J. Phys. Soc. Japan 26, 1473 (1969).

35. W. H. Miller, J. Chem. Phys. 52, 3563 (1970).

36. The factor $(2\hbar^2 k_*/\mu)^{5/6}$ in Eq. (45) of reference 35 should be $(2\hbar^2 k_*/\mu\varepsilon''_*)^{1/3}$.

37. M. J. Shaw, R. C. Bolden, R. S. Hemsworth and N. D. Twiddy, Chem. Phys. Letters 8, 148 (1971).

Table I. Autoionization Width versus Internuclear Distance[a]

	Internuclear Distance (Bohrs)			
	2	4	6	8
I_0[b]	-1.835×10^{-2}	-5.416×10^{-3}	7.282×10^{-4}	2.132×10^{-5}
I_1	1.846×10^{-2}	-3.977×10^{-3}	-1.921×10^{-3}	1.223×10^{-4}
I_2	-9.754×10^{-3}	1.012×10^{-2}	-9.878×10^{-4}	-4.941×10^{-4}
I_3		7.753×10^{-3}	1.421×10^{-3}	-2.772×10^{-4}
I_4		2.640×10^{-3}	1.748×10^{-3}	3.953×10^{-4}
I_5		5.275×10^{-4}	9.948×10^{-4}	6.714×10^{-4}
I_6			3.819×10^{-4}	5.375×10^{-4}
I_7				3.021×10^{-4}
I_8				1.341×10^{-4}
I_9				4.981×10^{-5}
ε[c]	0.334238	0.159524	0.197397	0.219123
Γ[d]	3.781×10^{-3}	1.522×10^{-3}	7.262×10^{-5}	8.122×10^{-6}

[a]All quantities are in atomic units.

[b]The matrix element $I_\ell(R)$ defined in Eq. (18).

[c]The asymptotic energy of the electron if autoionization occurs at R, $\varepsilon(R) \equiv V_o(R) - V_+(R)$.

[d]The total autoionization width at internuclear distance R, given by Eq. (23)-(24).

Figure Captions

Fig. 1. The potential energy curves for $He^*(1s2s\ ^3S)$-$H(1s\ ^2S)$ $^2\Sigma[V_o(R)]$ and $He(1s^2\ ^1S)$-$H^+\ ^1\Sigma[V_+(R)]$, as calculated in reference 15.

Fig. 2. The matrix elements $I_\ell(R)$ defined in Eq. (18) and calculated by the procedure described in Section II of the text; corresponding numerical values are given in Table I.

Fig. 3. The total autoionization width [given by Eqs. (23)-(24)] as a function of internuclear distance R; corresponding numerical values are given in Table I. The dashed curve is the result of Bell [reference 14] for this quantity.

Fig. 4. The asymptotic kinetic energy of the ionized electron as a function of the internuclear distance R at which autoionization occurs: $\varepsilon(R) \equiv V_o(R)-V_+(R)$, where $V_o(R)$ and $V_+(R)$ are the potential curves for He^*-H and He-H^+, respectively, as shown in Fig. 1. The dotted lines indicate the internuclear distance R_{AI} of Eq. (41)-(42) for which $\varepsilon(R) = \varepsilon(\infty)$.

Fig. 5. The total ionization cross section for $He^*(1s2s\ ^3S) + H(1s\ ^2S) \rightarrow He(1s^2\ ^1S) + H^+ + e^-$, $HeH^+(^1\Sigma) + e^-$ as a function of collision energy E; AI indicates the cross section for associated product HeH^+. The dashed lines are the results of the "scaled orbitting model", Eqs. (35)-(38).

Fig. 6. The percentage of the total ionization cross section which yields associated product HeH^+, as a function of collision energy. The zero energy limit of this quantity is 22%, the top border of the figure.

Fig. 7. $P_o(R)$ is the function $P_b(R)$ of Eq. (32) for the case b = E = 0; $P_o(R)dR$ is the probability that autoionizations occur for an internuclear distance in the interval (R, R+dR). R_o and R_{AI} are the roots of $V_o(R) = V_o(\infty)$ and $\varepsilon(R) = \varepsilon(\infty)$, respectively.

Fig. 8. $\tilde{P}_o(R)$ [defined by Eqs. (39)-(40)] is the probability that autoionization occurs at an internuclear distance less then or equal to R for the case that the impact parameter and collision energy are zero (b=E=0); the asymptotic ($R\to\infty$) value is $P_o = 0.789$. The positions R_o and R_{AI} are the roots of $V_o(R) = V_o(\infty)$ and $\varepsilon(R) = \varepsilon(\infty)$, respectively.

Fig. 9. The energy distribution of the ionized electron, $\sigma(\varepsilon)$, as computed from the classical expressions Eqs. (31) and (32), for the collision energy E = 0.01 eV. The dashed line indicates the semiclassical modification given by Eq. (34), and the arrow shows the location of $\varepsilon_* \simeq 4.32$ eV, the minimum of $\varepsilon(R)$.

Fig. 10. Same as Fig. 9, except for the collision energy E = 0.03 eV.

Fig. 11. Same as Fig. 9, except for the collision energy E = 0.136 eV.

Fig. 12. $P_o(\varepsilon)$, defined by Eq. (43), is the probability distribution of ε for the case that b = E = 0. The vertical lines at $\varepsilon \simeq 4.32$ eV and $\varepsilon \simeq 7.43$ eV are the values ε_* and $\varepsilon(R_o)$, respectively, where R_o is the zero-energy turning point for the potential $V_o(R)$.

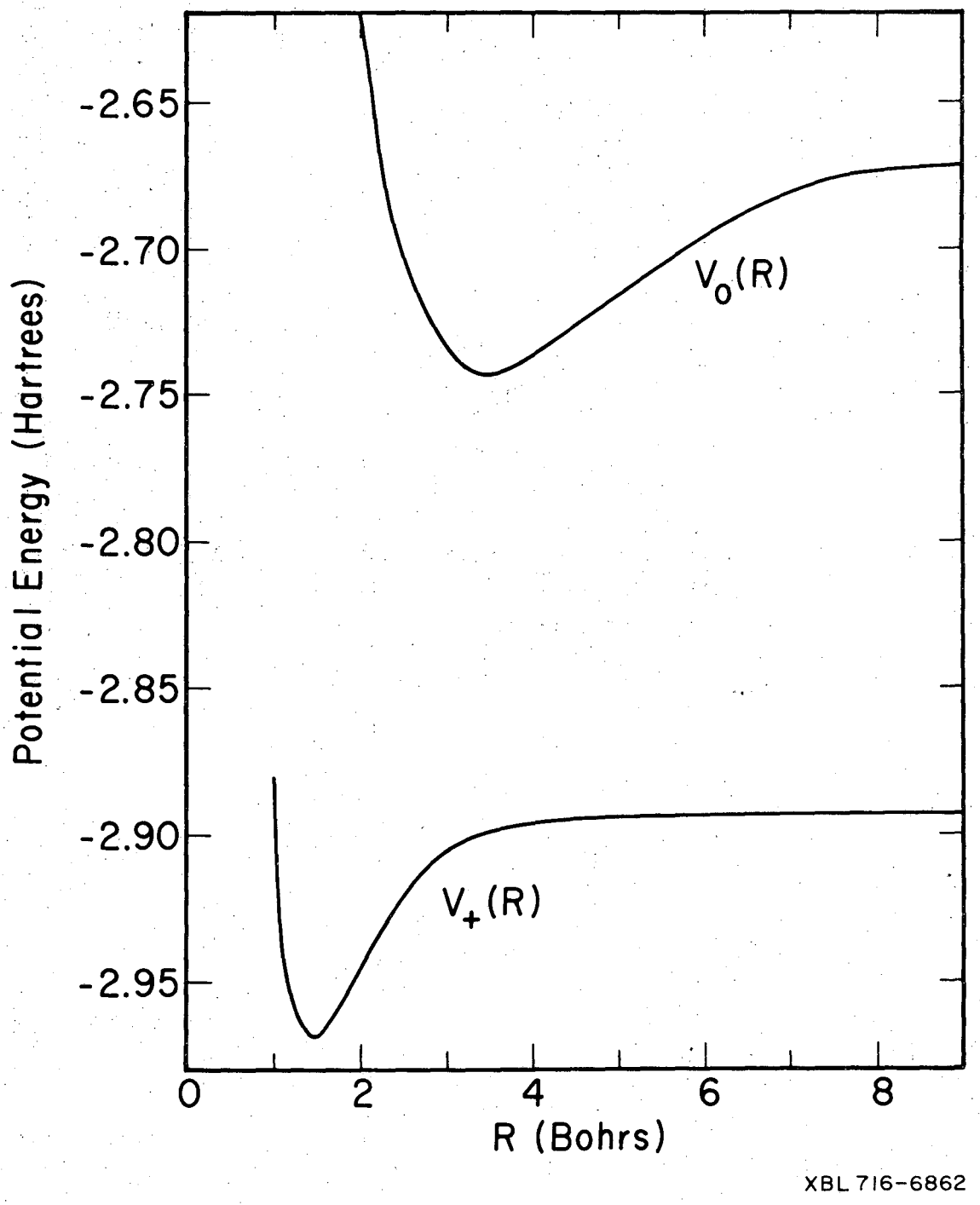
-2.65
-2.70
-2.75
-2.80
-2.85
-2.90
-2.95
Potential Energy (Hartrees)
$V_0(R)$
$V_+(R)$
0
2
4
6
8
R (Bohrs)
XBL 716-6862

Fig.1

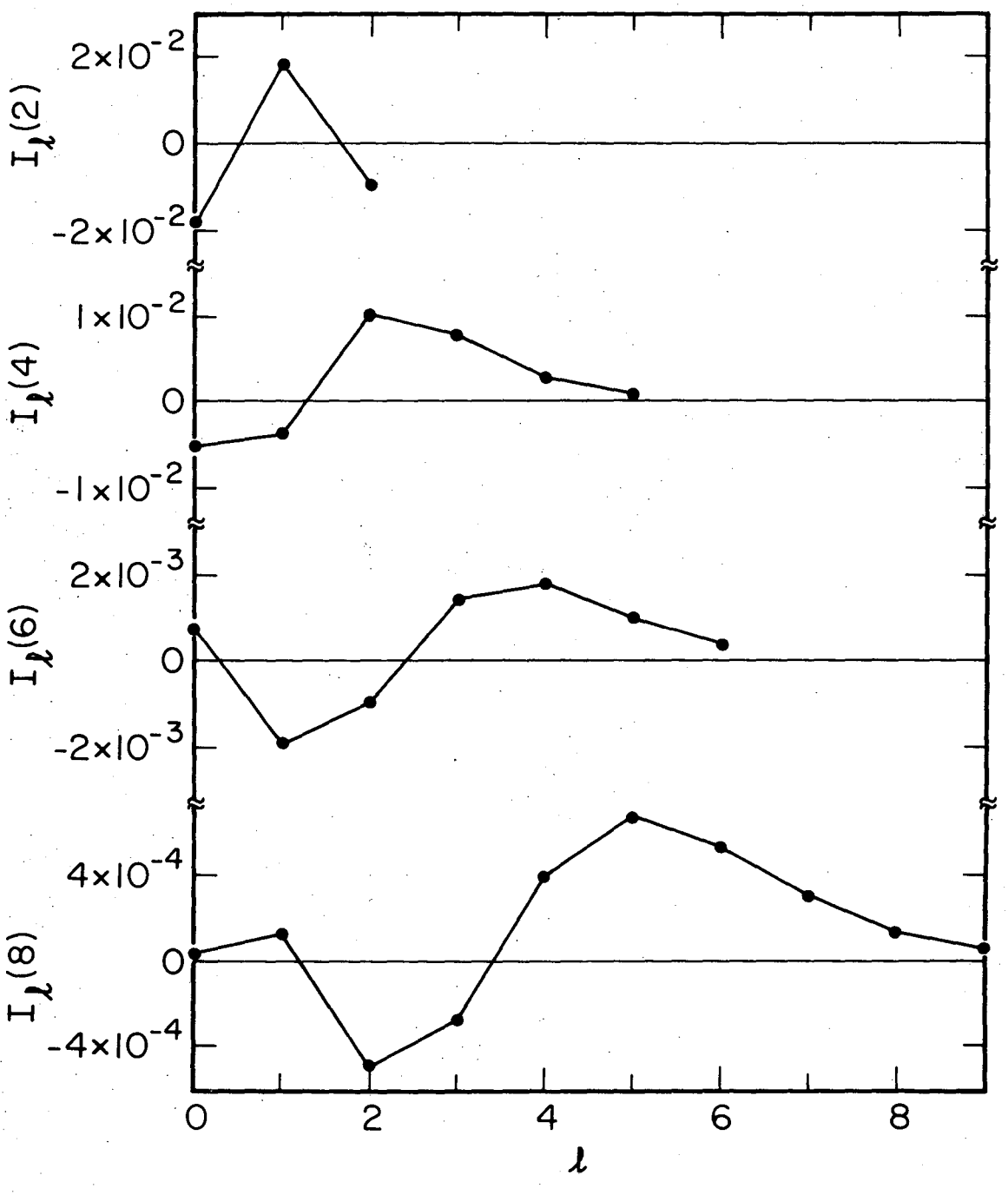
$I_\ell(2)$
2×10^{-2}
0
-2×10^{-2}
$I_\ell(4)$
1×10^{-2}
0
-1×10^{-2}
$I_\ell(6)$
2×10^{-3}
0
-2×10^{-3}
$I_\ell(8)$
4×10^{-4}
0
-4×10^{-4}
0
2
4
6
8
ℓ
XBL716-6863

Fig. 2

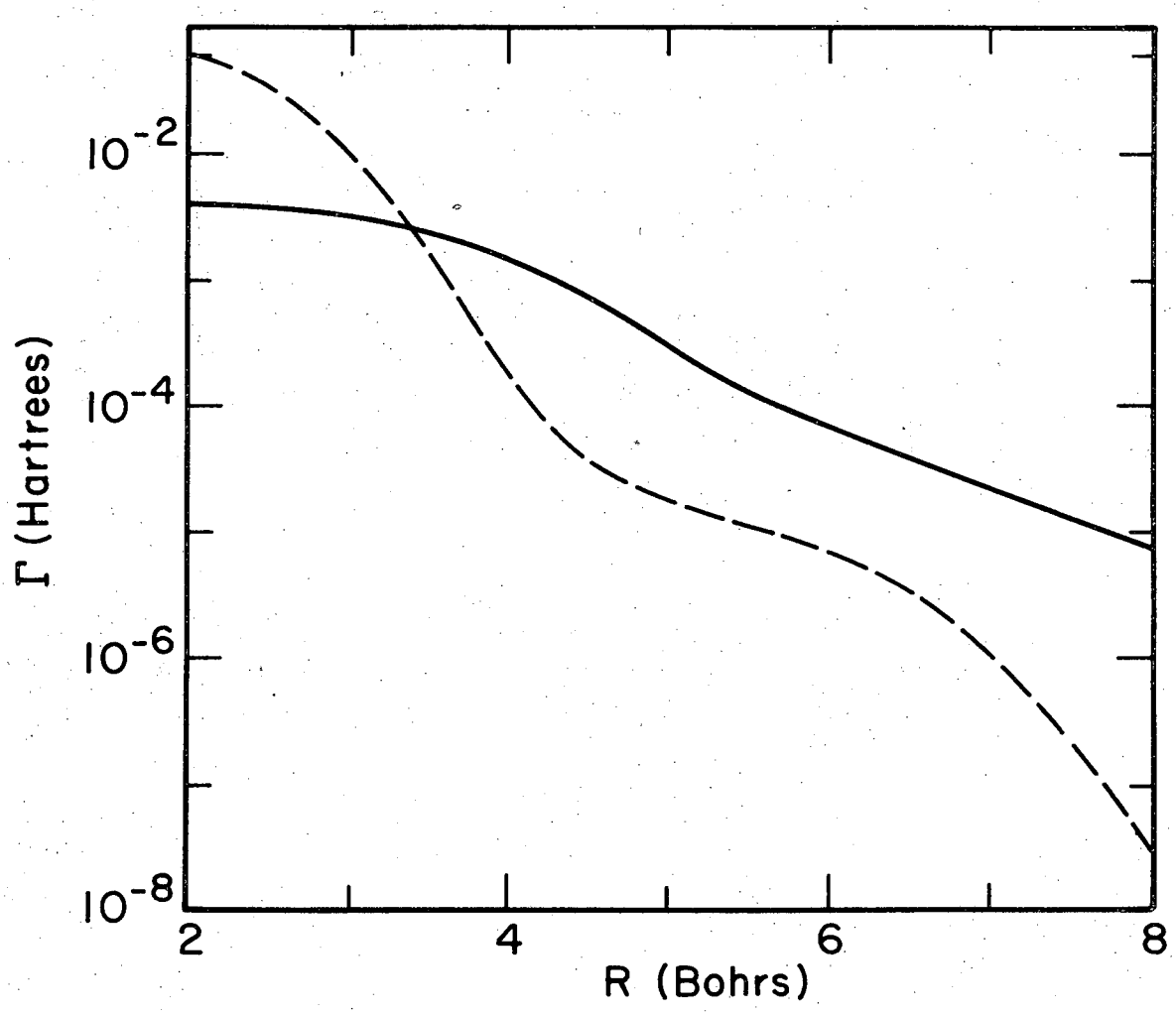

XBL 716-6860

Fig. 3

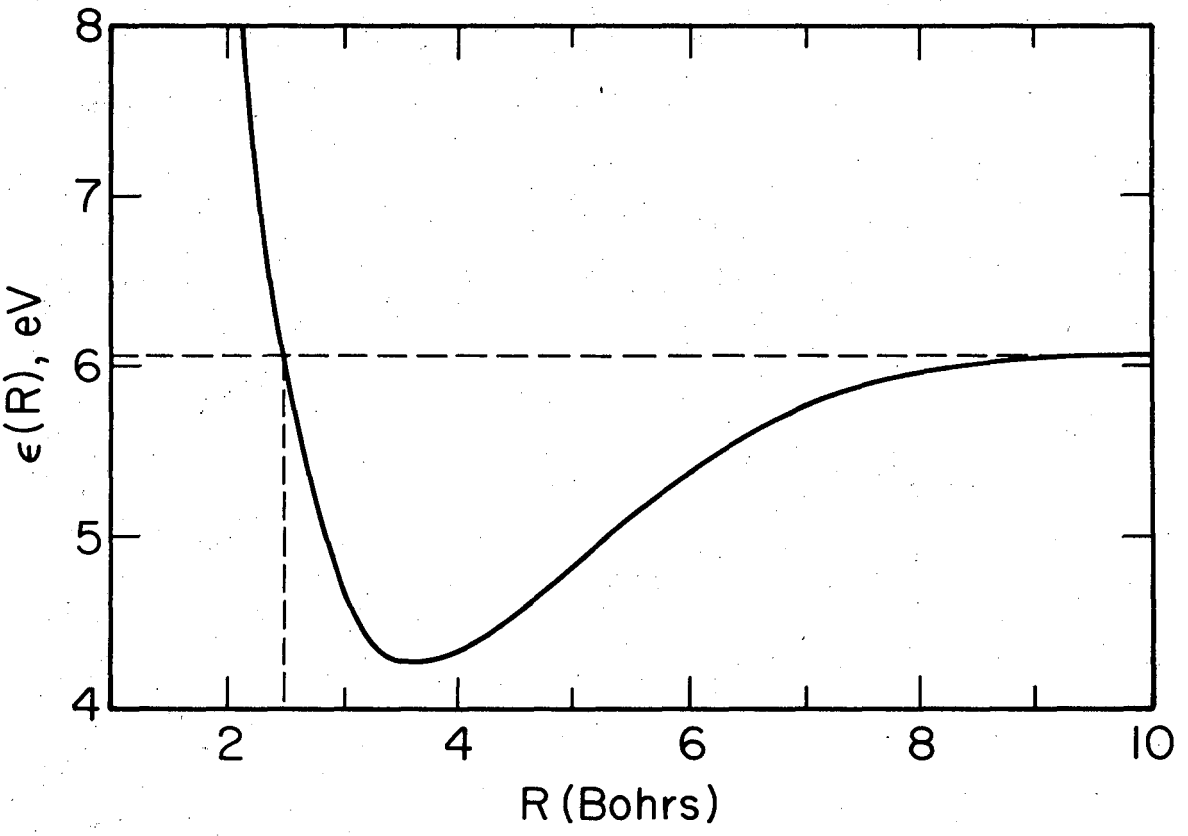

XBL 716-6861

Fig. 4

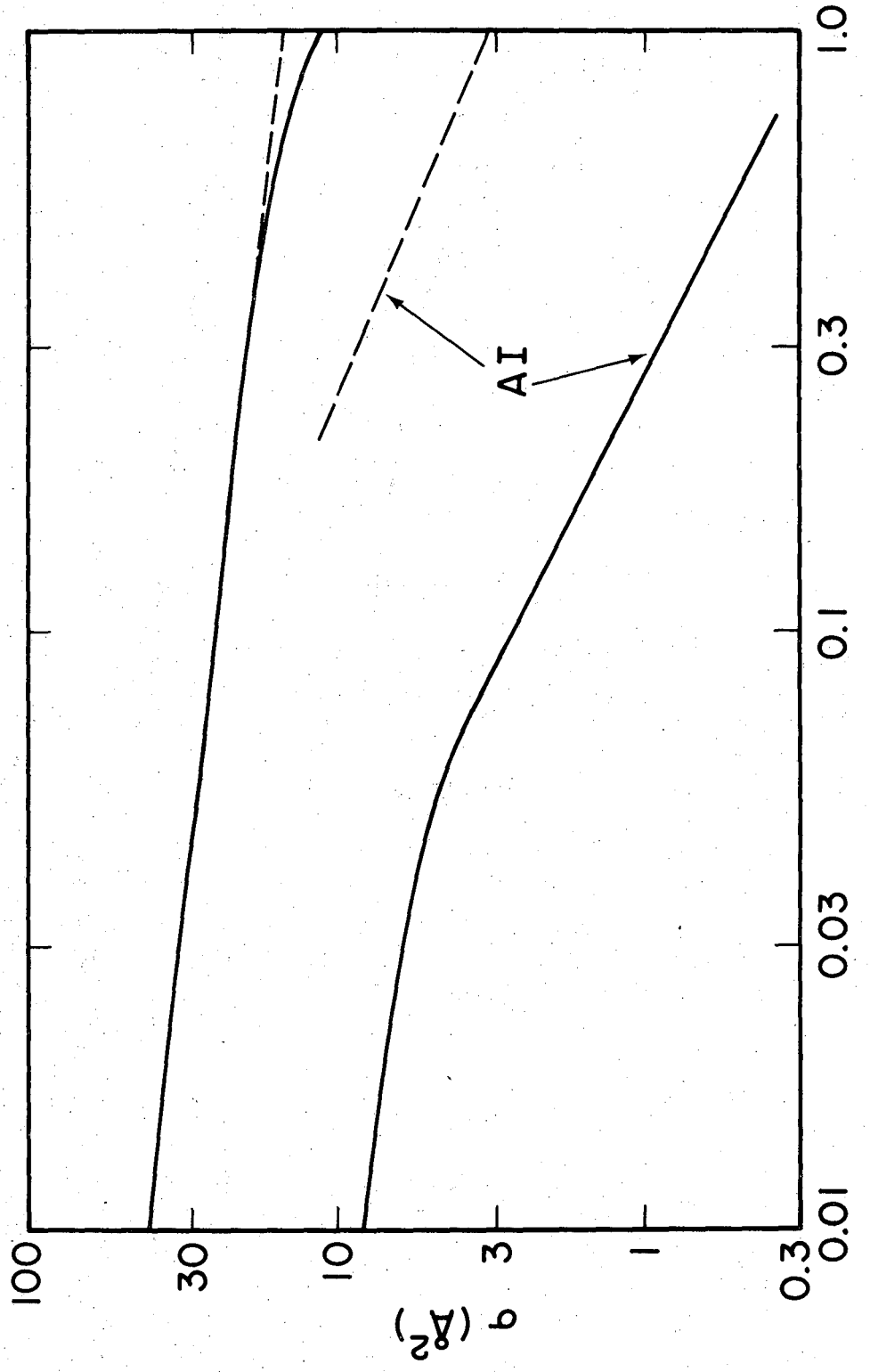

XBL 716-6859

Fig. 5

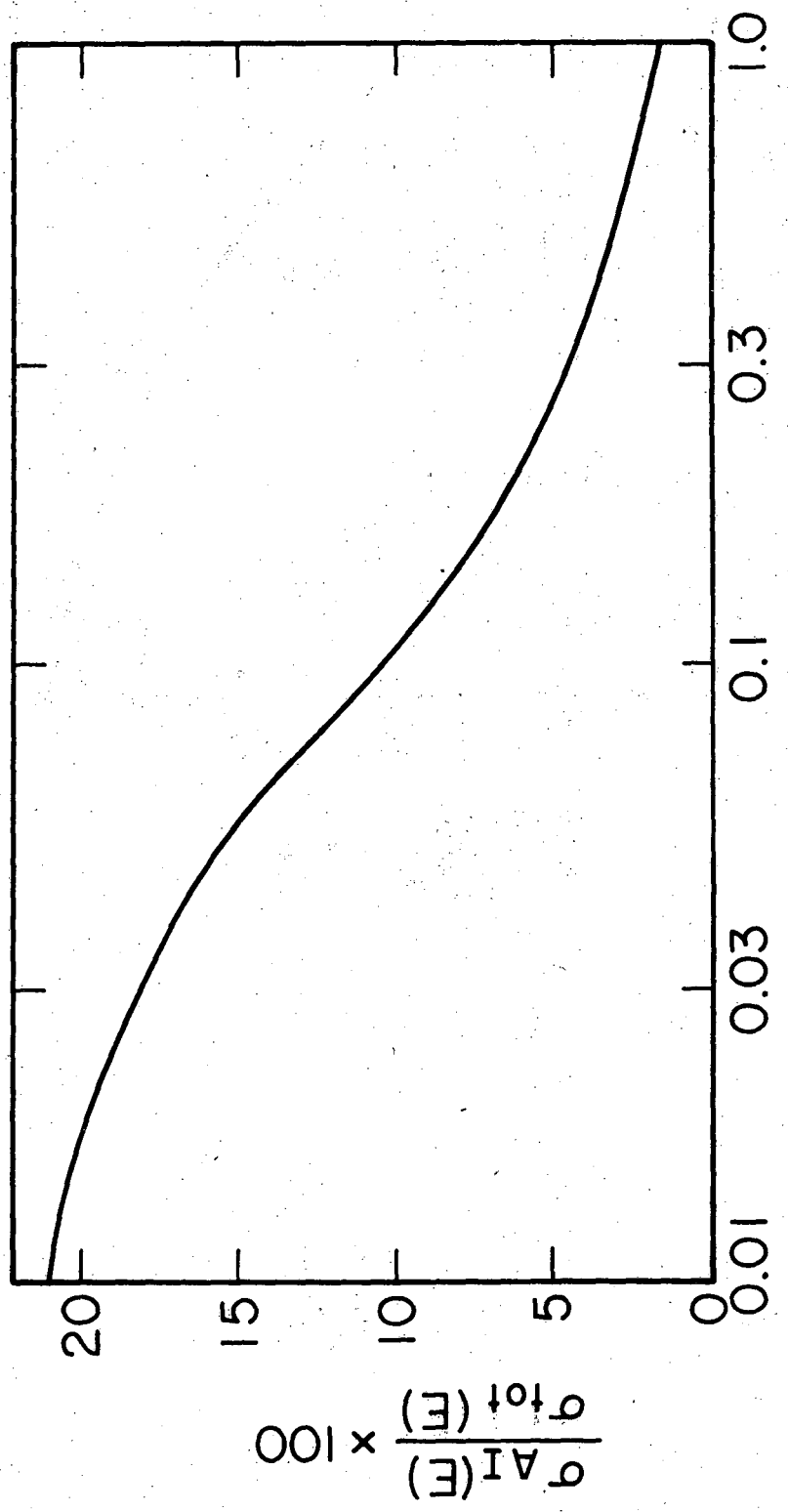

XBL 716-6858

Fig. 6

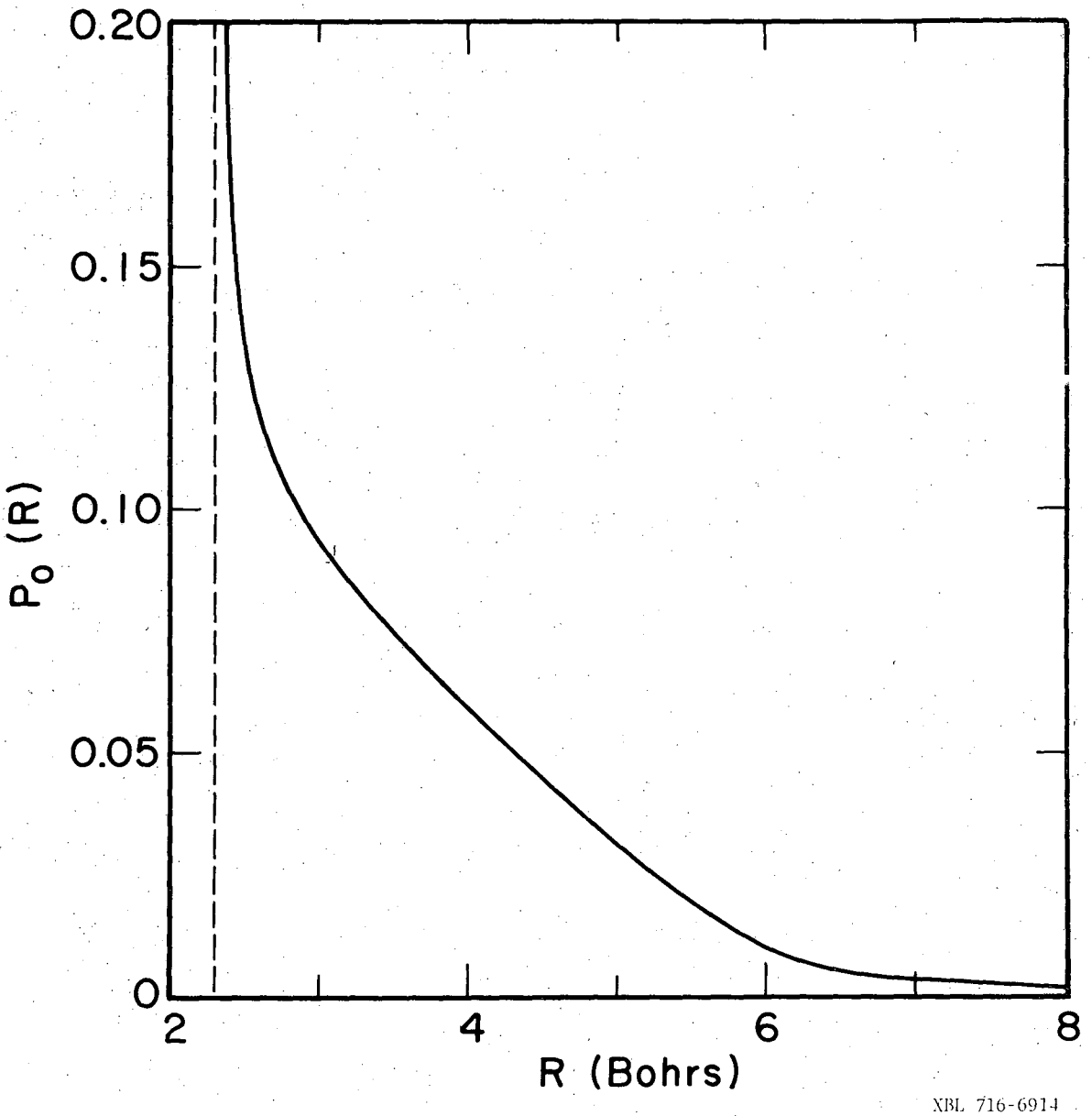

XBL 716-6914

Fig. 7

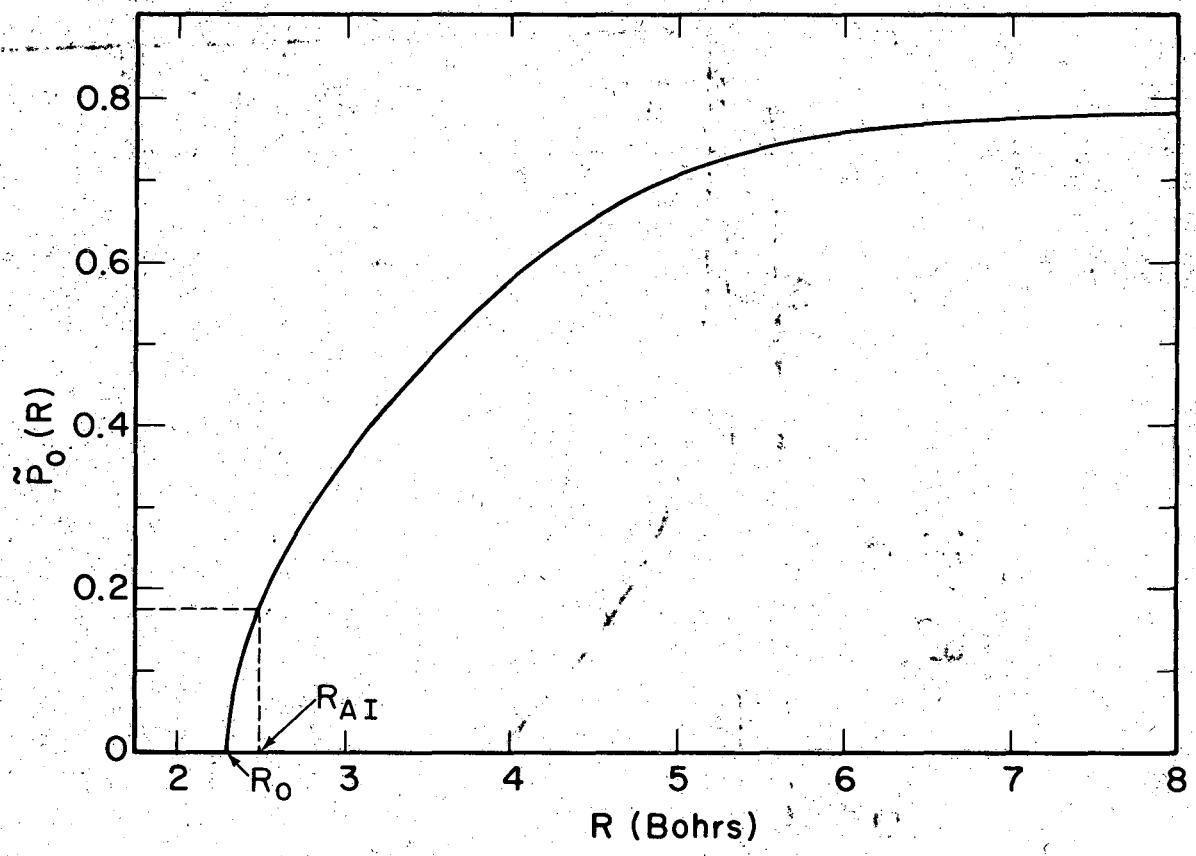

Fig. 8

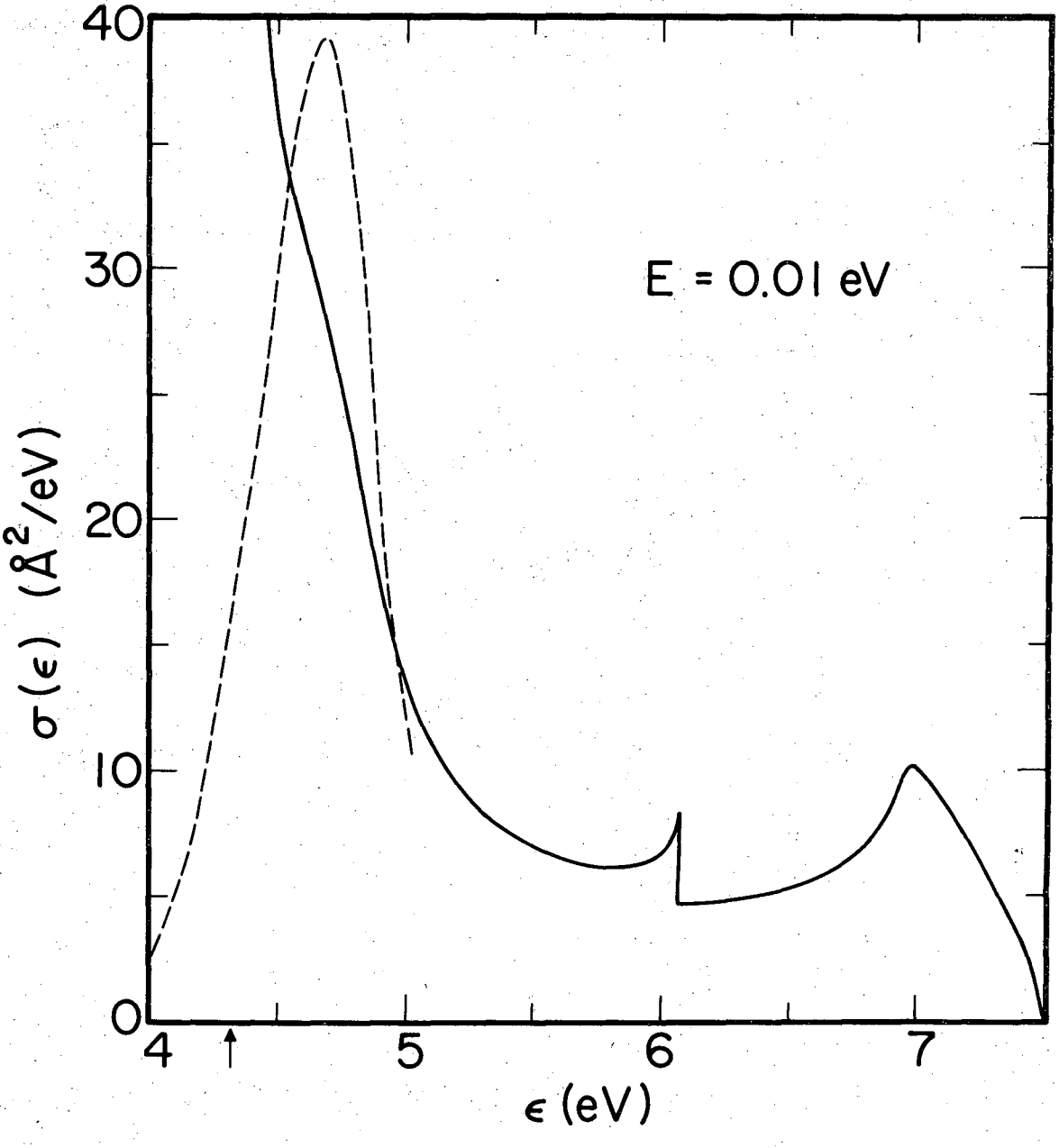

Fig. 9

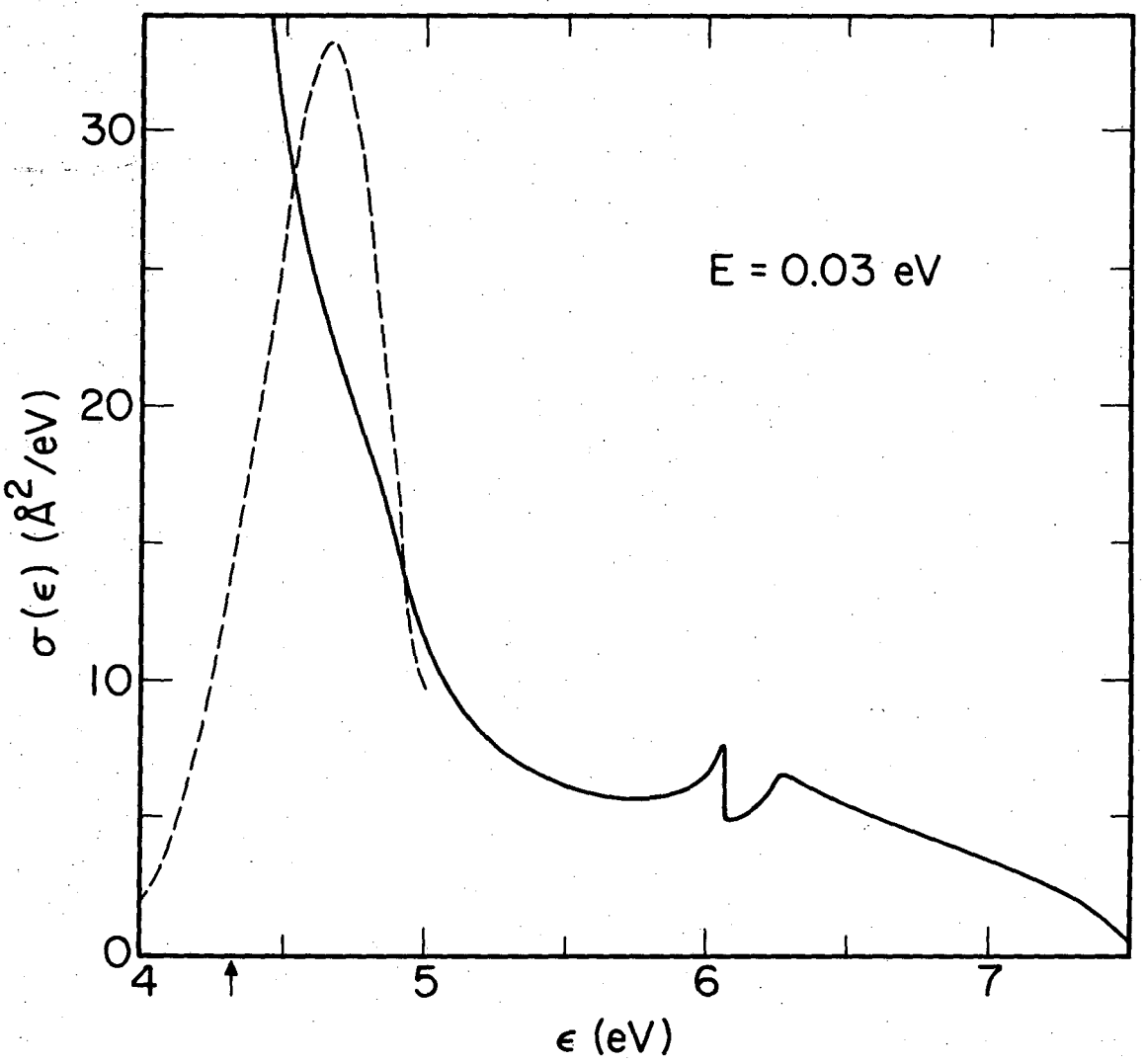

Fig. 10

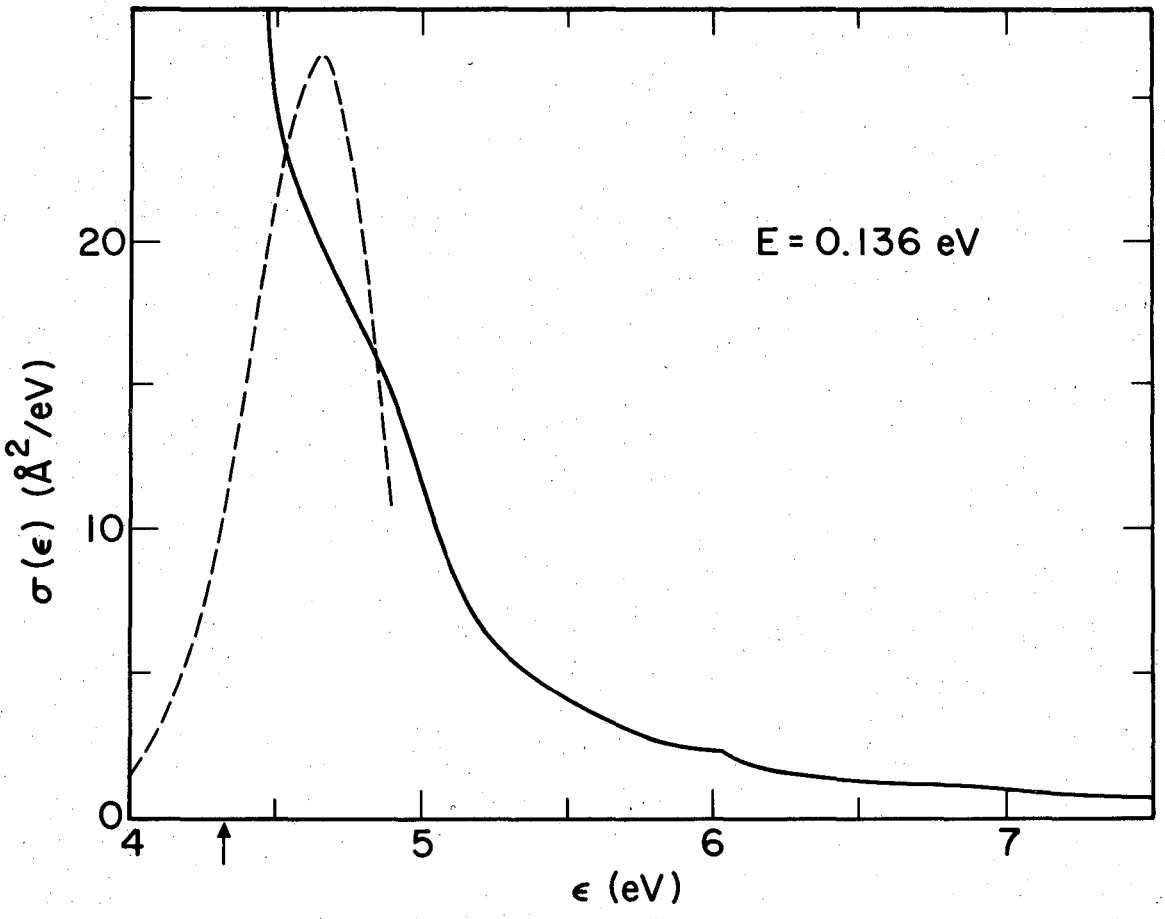

Fig. 11

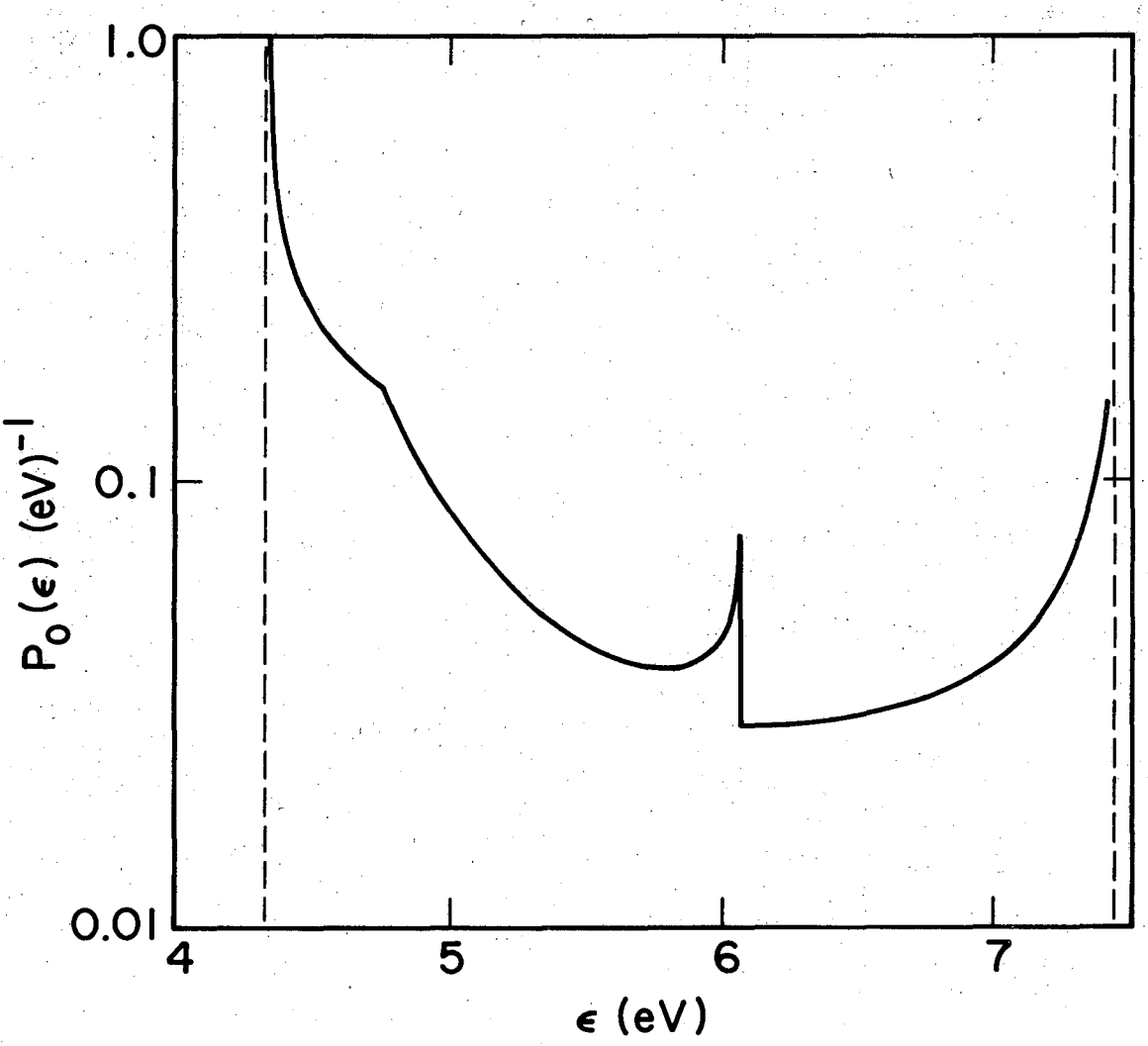

Fig. 12

TECHNICAL INFORMATION DIVISION
LAWRENCE BERKELEY LABORATORY
UNIVERSITY OF CALIFORNIA
BERKELEY, CALIFORNIA 94720